Article

Side-Chain Dynamics of an □-Helical Polypeptide Monitored by Fluorescence

Jean Duhamel, Sabesh Kanagalingam, Thomas J. O'Brie, and Mark W. Ingratta

J. Am. Chem. Soc., **2003**, 125 (42), 12810-12822• DOI: 10.1021/ja035947q • Publication Date (Web): 27 September 2003

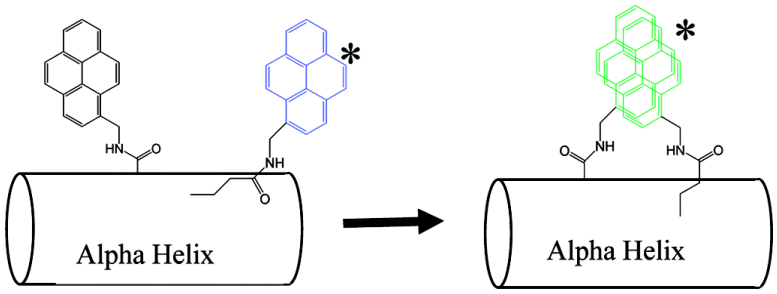

More About This Article

Additional resources and features associated with this article are available within the HTML version:

- Supporting Information
- Links to the 5 articles that cite this article, as of the time of this article download
- Access to high resolution figures
- Links to articles and content related to this article
- Copyright permission to reproduce figures and/or text from this article

View the Full Text HTML

J|A|C|S
ARTICLES
Published on Web 09/27/2003

Side-Chain Dynamics of an α-Helical Polypeptide Monitored by Fluorescence

Jean Duhamel,* Sabesh Kanagalingam, Thomas J. O'Brien, and Mark W. Ingratta

Contribution from the Institute for Polymer Research, Department of Chemistry, University of Waterloo, 200 University Avenue West, Waterloo, ON, N2L 3G1, Canada

Received May 5, 2003; E-mail: jduhamel@uwaterloo.ca

Abstract: The "blob" model, developed to analyze the fluorescence decays of polymers randomly labeled with pyrene, has been applied to a series of pyrene-labeled poly(glutamic acid)s (PyPGA) in DMF and carbonated buffer solutions at pH 9. Poly(glutamic acid) (PGA) exists in the ionized form in the buffer solutions as poly(sodium glutamate) (PGNa). PGA adopts an α-helical conformation in DMF, whereas in aqueous solution PGNa is a random coil. Fluorescence, UV−vis absorption, and circular dichroism measurements indicate that in our studies pyrene pendants attached themselves along PGA in a clustered manner. Simulations were carried out to establish that the geometry of the PGA α-helix induces the high level of pyrene clustering. Since the level of pyrene clustering decreased with lower pyrene content, information about naked PGA was retrieved by extrapolating the trends obtained by fluorescence to zero pyrene content. Analysis of the fluorescence decays demonstrated that during its lifetime an excited pyrene probes a 32 amino acid section of the PGA α-helix. This result was supported by molecular mechanics optimizations. This study establishes that the *blob* model, originally used to monitor the encounters between pyrenes attached randomly onto a polymer adopting a random coil conformation, can also be applied to study the dynamics of the side chains of structured proteins. Since the *blob* model helps in monitoring the encounters between amino acids in the initial state (i.e., random coil) and in the final state (i.e., structured protein) of the folding pathway of a protein, it could be applicable to the study of protein folding.

Introduction

To this date, the study of the diffusional encounters taking place between pendants attached onto a polymer chain has mainly focused on very well-defined polymeric systems where two fluorescent tags are attached at specific positions spanning an equal distance along the chain. In a typical experiment, a fluorescent pendant and its quencher are attached at both ends of a monodisperse polymer. The rate at which the fluorescent pendant is being quenched yields information about the end-to-end cyclization rate. A large body of theoretical[1] and experimental[2] work was generated within this framework which established that the end-to-end cyclization rate depends strongly on the chain length spanning the dye and its quencher. Such conclusions made it difficult to study in a quantitative manner the encounters taking place between pendants randomly distributed along the backbone of a polydisperse polymer, because the random attachment of the pendants along the polymer chain leads to a distribution of chain lengths spanning every two pendants, which in turn yields an intractable distribution of rates of encounter. This was an unfortunate situation because pendants randomly attached onto a polymer backbone can probe the entire polymer chain instead of just the two ends as in an end-to-end cyclization study. Furthermore, the ability to *quantitatively* characterize how pendants attached along a polymeric backbone encounter each other would certainly be beneficial to the study of associative polymers or the folding of proteins, two polymeric systems where pendants or side chains distributed along the polymer chain interact with one another.

These considerations prompted us to propose an analytical tool coined the "blob" model, which allows for the study of encounter and association of fluorescent pendants attached randomly onto the backbone of polymers.[3−7] Pyrene was chosen

(1) Ortiz-Repiso, M.; Freire, J. J.; Rey, A. *Macromolecules* **1998**, *31*, 8356−8362. Rey, A.; Freire, J. J.; Garcia de la Torre, J. *Polymer* **1992**, *33*, 3477. Friedman, B.; O'Shaughnessy, B. *J. Phys. II* **1991**, *1*, 471−486. Perico, A.; Cuniberti, C. *J. Polym. Sci. Polym. Phys. Ed.* **1977**, *15*, 1435−1450. de Gennes, P. G. *J. Chem. Phys.* **1982**, *76*, 3316−3321. Wilemski, G.; Fixman, M. *J. Chem. Phys.* **1973**, *58*, 4009−4019. Wilemski, G.; Fixman, M. *J. Chem. Phys.* **1974**, *60*, 878−890. Doi, M. *Chem. Phys.* **1975**, *9*, 455−466. Doi, M. *Chem. Phys.* **1975**, *11*, 115−121. Garcia Fernández, J. L.; Rey, A.; Freire, J. J.; Fernández de Piérola, I. *Macromolecules* **1990**, *23*, 2057−2061. Rey, A.; Freire, J. J. *Macromolecules* **1991**, *24*, 4673−4678. Friedman, B.; O'Shaughnessy, B. *Macromolecules* **1993**, *26*, 4888−4898. Perico, A.; Beggiato, M. *Macromolecules* **1990**, *23*, 797−803. Rubio, A. M.; Pita, M.; Freire, J. J. *Macromolecules* **2002**, *35*, 5681−5687.

(2) Cuniberti, C.; Perico, A. *Eur. Polym. J.* **1977**, *13*, 369−374. Winnik, M. A.; Redpath, T.; Richards, D. H. *Macromolecules* **1980**, *13*, 328−335. Redpath, A. E. C.; Winnik, M. A. *J. Am. Chem. Soc.* **1980**, *102*, 6869−6871. Redpath, A. E. C.; Winnik, M. A. *J. Am. Chem. Soc.* **1982**, *104*, 5604−5607. Winnik, M. A.; Sinclair, A. M.; Beinert, G. *Can. J. Chem.* **1985**, *63*, 1300−1307. Winnik, M. A.; Redpath, A. E. C.; Paton, K.; Danhelka, J. *Polymer*, **1984**, *25*, 91−99. Martinho, J. M. G.; Winnik, M. A. *Macromolecules* **1986**, *19*, 2281−2284. Martinho, J. M. G.; Reis e Sousa, A. T.; Winnik, M. A. *Macromolecules* **1993**, *26*, 4484−4488. Reis e Sousa, A. T.; Castanheira, E. M. S.; Fedorov, A.; Martinho, J. M. G. *J. Phys. Chem. A* **1998**, *102*, 6406−6411. Kane, M. A.; Baker, G. A.; Pandey, S.; Maziarz, E. P., III; Hoth, D. C.; Bright, F. V. *J. Phys. Chem. B* **2000**, *104*, 8585−8591.

(3) Mathew, A. K.; Siu, H.; Duhamel, J. *Macromolecules* **1999**, *32*, 7100−7108.

(4) Kanagalingam, S.; Ngan, C. F.; Duhamel, J. *Macromolecules* **2002**, *35*, 8560−8570.

(5) Kanagalingam, S.; Spartalis, J.; Cao, T.-M.; Duhamel, J. *Macromolecules* **2002**, *35*, 8571−8577.

(6) Vangani, V.; Duhamel, J.; Nemeth, S.; Jao, T.-C. *Macromolecules* **1999**, *32*, 2845−2854. Vangani, V.; Drage, J.; Mehta, J.; Mathew, A. K.; Duhamel, J. *J. Phys. Chem. B.* **2001**, *105*, 4827−4839.

10.1021/ja035947q CCC: $25.00

as the fluorescent probe. Upon excitation with UV light, pyrene becomes excited and can either fluoresce with its natural lifetime (τ_M, usually in the 200−300 ns range) in the blue region of the visible light spectrum or encounter another ground-state dye and form a bimolecular species called an excimer.[8] The excimer also fluoresces with its natural lifetime (τ_{E0}, usually in the range of 45−55 ns) in the green region of the visible light spectrum.[4−7] In the framework of the blob model, a blob is the volume that an excited pyrene probes during its lifetime.[3−7] This generates a unit volume which can be used to divide the polymer coil into blobs. If the polymer chain is randomly labeled with pyrene, the pyrene molecules distribute themselves randomly among the blobs according to a Poisson distribution. The kinetics of encounter taking place between one excited pyrene and ground-state pyrenes randomly distributed among blobs are similar to those observed with micellar systems.[9] They are described by three parameters. These are the average number of pyrene groups per blob, $\langle n \rangle$, the rate constant of excimer formation inside a blob containing one excited pyrene and one ground-state pyrene only, k_{blob}, and the rate at which pyrene groups exchange between blobs, k_e[blob]. Here, k_e is the exchange rate constant and [blob] is the blob concentration inside the polymer coil. Work from this laboratory has demonstrated the validity of the blob model at describing the dynamics of encounters between pendants randomly attached onto a polymer backbone. Examples of polymers studied include polystyrene,[3] poly(*N*,*N*-dimethylacrylamide) (PDMAAm),[4,5] ethylene−propylene copolymer,[6] and polymers where pyrene is attached by a long tether onto the main chain.[7]

The above examples dealt with polymers adopting a random-coil conformation in solution. In terms of protein folding, one can consider this state as the early stage of the folding of a polypeptide, when the unfolded chain is stretched in solution. For polypeptides though, encounters between the amino acid side chains start to occur, leading to the formation of secondary structures such as α-helices and β-sheets, which further rearrange to yield the final three-dimensional structure of the protein.[10] Certainly, the claim that the blob model can be a useful tool for the study of protein folding would be strengthened if its ability at describing the encounters between pendants attached onto a polymer chain could be extended from random-coil polymers to polymers adopting a secondary structure. To this end, we initiated a study aimed at characterizing the encounters taking place between pyrene groups randomly attached onto poly(L-glutamic acid) (PGA). PGA was chosen for two reasons. First, it is a polypeptide that contains an acid functionality which allows for easy attachment of 1-pyrenemethylamine. Second, it has been shown to adopt a helical structure in the acidic form stabilized by hydrogen bonding in the main chain and a random coil conformation in a buffer solution under alkaline conditions.[11] The ability of PGA to undergo a helix-to-coil transition renders it a model system to study, both experimentally[12a] and theoretically,[12b] protein folding and unfolding. Since pyrene is a hydrophobic molecule, the pyrene-labeled PGA (PyPGA) was studied in *N*,*N*-dimethylformamide (DMF) as a substitute for water in order to prevent the pyrene associations observed in aqueous solutions. DMF is described as a helicogenic solvent[13] where PGA is known to adopt an α-helical geometry.[14] Furthermore, the good solubility of pyrene molecules in DMF ensures that pyrene−pyrene interactions would not induce a perturbation of the rigid rod conformation adopted by PGA. Pyrene was randomly attached onto the PGA backbone via carbodiimide coupling of 1-pyrenemethylamine and glutamic acid. The presence of pyrene groups along the PGA backbone is not expected to alter the α-helical geometry of the polypeptide as demonstrated by circular dichroism experiments carried out on fully and partially pyrene-labeled PGAs in *N*,*N*-dimethylacetamide, a solvent whose structure and characteristics are very similar to that of DMF.[15]

Table 1. Pyrene Content in mol % and λ (Moles of Pyrene per Gram of Polymer), P_A of Py-PGA in DMF and Buffer Solutions[a]

polymer name	λ (μmol·g^{-1})	mol %	P_A(DMF)	P_A(buffer)
30-PyPGA[b]	30	0.4		
70-PyPGA	70	0.9	2.4	2.1
180-PyPGA	180	2.4	2.5	1.7
300-PyPGA	300	4.0	2.5	1.6
420-PyPGA	415	5.5	2.5	1.5
520-PyPGA	515	6.9	2.5	1.3
560-PyPGA	565	7.5	2.6	1.3
670-PyPGA	670	9.0	2.5	1.1
720-PyPGA	715	9.5	2.4	1.1
860-PyPGA	860	11.4	2.4	1.1
880-PyPGA	885	11.8	2.4	1.1

[a] Buffer refers to 0.01 M aqueous carbonate buffer at pH = 9.0 with 0.05M NaCl. [b] Not enough sample to measure P_A accurately.

Several pyrene-labeled PGA samples were prepared with pyrene contents ranging from 0.4 to 11.8 mol % as listed in Table 1. The polymers were studied in the protonated form in DMF and in the ionized form (sodium salt, PGNa) at pH 9 in an aqueous carbonate buffer solution. The dynamics of the encounter and association of the pyrenes attached onto PGA and PGNa were examined in detail. Since PGA adopts a helical conformation in DMF, the encounters between the pyrene groups represent the motions of the side chains of the amino acids anchored along the rigid rod. Of particular interest is the comparison between the results obtained with pyrene-labeled PDMAAm[4,5] (a random coil in DMF) and PGA (a rigid rod in DMF).

Special emphasis in the discussion of the results is given to those obtained with PyPGA in DMF, because PGA in DMF adopts an α-helical conformation[14] and also because the results obtained with PyPGNa in aqueous solutions were more difficult to interpret due to the presence of hydrophobic pyrene ag-

(7) Prazeres, T. J. V.; Beingessner, R.; Duhamel, J.; Olesen, K.; Shay, G.; Bassett, D. R. *Macromolecules* **2001**, *34*, 7876−7884.
(8) Birks, J. B. *Photophysics of Aromatic Molecules*; Wiley: New York, 1970; pp 301−371.
(9) (a) Infelta, P. P.; Gratzel, M.; Thomas, J. K. *J. Phys. Chem.* **1974**, *78*, 190−195. (b) Tachiya, M. *Chem. Phys. Lett.* **1975**, *33*, 289−292.
(10) Fersht, A. R. *Curr. Opin. Struct. Biol.* **1997**, *7*, 3−9. Volk, M. *Eur. J. Org. Chem.* **2001**, 2605−2621.
(11) Doty, P.; Wada, A.; Yang, J. T.; Blout, E. R. *J. Polym. Sci.* **1957**, *23*, 851−861. Idelson, M.; Blout, E. R. *J. Am. Chem. Soc.* **1958**, *80*, 4631−4634. Yamaoka, K.; Ueda, K.; Asato, M. *J. Am. Chem. Soc.* **1984**, *106*, 3865−3866.
(12) (a) Nagasawa, M.; Holtzer, A. *J. Am. Chem. Soc.* **1964**, *86*, 538−543. Olander, D. S.; Holtzer, A. *J. Am. Chem. Soc.* **1968**, *90*, 4549−4560. Martin, P. W.; Kalfas, C. A.; Skov, K. *Chem. Phys. Lett.* **1978**, *57*, 279−280. Noji, S.; Nomura, T.; Yamaoka, K. *Macromolecules* **1980**, *13*, 1114−1120. Kidera, A.; Nakajima, A. *Macromolecules* **1984**, *17*, 659−663. Satoh, M.; Fujii, Y.; Kato, F.; Komiyama, J. *Biopolymers* **1991**, *31*, 1−10. Zhang, W.; Nilsson, S. *Macromolecules* **1993**, *26*, 2866−2870. (b) Zimm, B. H.; Gragg, J. K. *J. Chem. Phys.* **1959**, *31*, 526−535. Zimm, B. H.; Rice, S. A. *Mol. Phys.* **1960**, *3*, 391−407.
(13) Norisuye, T.; Teramoto, A.; Fujita, H. *Polym. J.* **1973**, *4*, 323−331.
(14) Yamaoka, K.; Ueda, K. *J. Phys. Chem.* **1982**, *86*, 406−413.
(15) Shoji, O.; Okumura, M.; Kuwata, H.; Sumida, T.; Kato, R.; Annaka, M.; Yoshikuni, M.; Nakahira, T. *Macromolecules* **2001**, *34*, 4270−4276.

Scheme 1. Pyrene Labeling of Poly(glutamic acid)

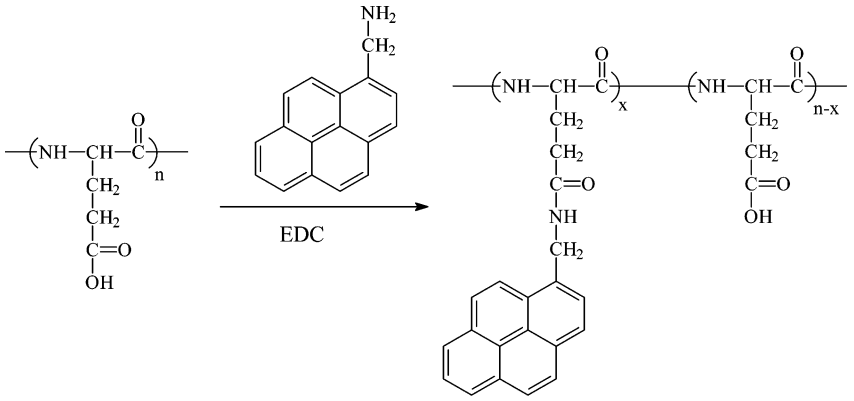

gregates. In terms of application to protein folding, experiments performed in water would certainly be preferable to DMF. Unfortunately, options in terms of solvent are limited by the nonsolubility of the tag of choice (i.e., pyrene) in water for the type of studies carried out in this work. Consequently the conclusions reached in this Article hold for the folding of proteins in DMF, admittedly a simpler case than water. It is our hope that the conclusions with DMF will also hold for the folding of protein in water, but at this stage, application of this approach to the more complex problem of protein folding in aqueous solution is still a matter of investigation.

Experimental Section

All chemicals other than common solvents were purchased from Sigma-Aldrich (Milwaukee, WI) except for sodium dodecyl sulfate (SDS) which was purchased from VWR (Toronto, ON). Solvents (HPLC grade or better) were purchased from Sigma-Aldrich or VWR and used interchangeably. All solvents were used as received unless otherwise noted. Doubly distilled water (deionized from Millipore Milli-RO 10 Plus and Milli-Q UF Plus (Bedford, MA)) was used in all preparatory steps and spectroscopy experiments. PGNa was purchased from Sigma-Aldrich which provided the following information: DP-(viscosity) = 363, MW(viscosity) = 54 800, DP (LALLS) = 241, MW (LALLS) = 36 400, M_w/M_n (SEC-LALLS) = 1.15.

Pyrene Labeling. 1-Pyrenemethylamine ($PyMeNH_2$) was obtained from the neutralization of 1-pyrenemethylamine hydrochloride (Aldrich) with NH_4OH in water and was extracted into hexane and washed and dried over NaOH pellets prior to use. PGNa (0.04 g) was placed in a 20 mL vial to which 3 mL of water was added. The solution was stirred, and 8 mL of DMF was further added. Various amounts of carefully weighed $PyMeNH_2$ were added directly to the solution (3×10^{-5} to 86×10^{-5} mol of Py/g of polymer), and the solution was vigorously stirred for approximately 15 min. One equivalent (3×10^{-5} to 86×10^{-5} mol of Py/g of polymer) of 1-[3-(dimethylamino)propyl]-3-ethylcarbodiimide hydrochloride (EDC) was then added. The reaction was carried out according to Scheme 1 under vigorous stirring for 5 h.

The reaction mixture was dialyzed with 3500MW cutoff dialysis bags against slightly acidic (1 day), basic (1 day), and neutral water (2 days) in subsequent steps for each polymer sample. The dialysis bags were emptied, and the recovered solution was dried with a rotatory evaporator, redissolved in water, and dried under vacuum: 300 MHz ^1H NMR (D_2O) δ in ppm 1.8 (broad doublet, ~2H, CH_2), 2.2 (broad doublet, ~2H, CH_2), 4.2 (broad, ~1H, CH), 4.6 (broad, ~1H, NH), and 7.5−8.4 (several peaks, pyrenyl H). The CH_2 adjacent to the pyrene peak usually observed at δ 5.2 ppm was not seen in most cases (<6 mol %). UV−vis absorbance (0.05M SDS in water): distinctive pyrene peaks at 344, 328, and 314 nm.

Determination of Pyrene Content (λ). A Hewlett-Packard 8452A diode array spectrophotometer was used for the absorption measurements. The spectrophotometer has an accuracy of at most ±1 nm. The pyrene content of the polymer was determined by measuring the absorbance of a solution prepared from a carefully weighed amount (m) of pyrene-labeled PGA in a known volume of DMF (V). The PGA was prepared from the PGNa by acidifying it with a few drops of 1 M HCl. It was dried in a vacuum oven at 40 °C for 30 min prior to use. DMF is a good solvent for pyrene, thus no significant pyrene−pyrene interactions are expected in this solvent, resulting in negligible distortion of the pyrene absorbance bands. The pyrene concentration [Py] in $mol \cdot L^{-1}$ was then calculated from the absorbance value at 344 nm using the value of 40 000 $mol^{-1} \cdot L \cdot cm^{-1}$ for the extinction coefficient of *N*-(1-pyrenylmethyl)acrylamide in DMF. The pyrene content λ expressed in mole of pyrene per gram of polymer ($mol \cdot g^{-1}$) was calculated from $\lambda = [Py]/(m/V)$. The absorbance spectra of PyPGNa in water and PyPGA in DMF were analyzed to qualitatively determine the amount of aggregation between pyrene pendants using the peak-to-valley ratio, P_A.[16]

Steady-State Fluorescence Measurements. These measurements were carried out on a Photon Technology International LS-100 steady-state system with a pulsed xenon flash lamp as the light source. All spectra were obtained with the usual right angle configuration. The samples had a pyrene concentration of 3×10^{-6} M to avoid intermolecular excimer formation. To prevent quenching of the pyrene fluorescence by dissolved oxygen, all samples were degassed for 20 min with a gentle flow of nitrogen. The fluorescence spectra were acquired by exciting the samples at 344 nm. The fluorescence intensities of the monomer (I_M) and the excimer (I_E) were calculated by taking the integrals under the fluorescence peaks from 372 to 378 nm for the pyrene monomer and from 500 to 530 nm for the pyrene excimer. Although the excimer maximum intensity was near 490 nm, the excimer intensity at wavelengths above 500 nm was considered to avoid potential overlap with the pyrene monomer fluorescence.

Time-Resolved Fluorescence Measurements. The time-dependent fluorescence decay profiles were obtained by the Time-Correlated Single Photon Counting (TCSPC) technique. Further information about this instrumentation can be found in earlier publications.[3] All polymer samples were excited at 344 nm, and the fluorescence was collected at 375 nm for the monomer decays and 510 nm for the excimer decays. As in other studies, the assumed function $g(t)$ for the fluorescence decays was convoluted with the instrument response function to fit the experimental decay.[3−7] A light scattering correction was applied to the fluorescence analysis to account for residual light scattering reaching the detector, as well as for those pyrenes attached close to one another which form excimer on a subnanosecond time scale, too short to be detected by our time-resolved fluorometer.[17] Several $g(t)$ functions were used. First the decays were fitted with a sum of exponentials with an expression given in eq 1 where the number of exponentials n is varied

(16) Winnik, F. M. *Chem. Rev.* **1993**, *93*, 587−614.
(17) Demas, J. N. *Excited-State Lifetime Measurements*; Academic Press: New York, 1983; p 134.

from 1 to 3. The index X in eq 1 is either M or E for the monomer or the excimer, respectively. The parameters of $g(t)$ were retrieved by using a least-squares curve fitting program based on the Marquardt−Levenberg algorithm.[18]

$$g(t) = \sum_{\substack{i=1 \\ X=M,E}}^{i=n} A_{Xi} e^{-t/\tau_{Xi}} \quad (1)$$

The monomer fluorescence decays were also fitted by the function $g(t)$ given by eq 2 which handles the kinetics of encounter between pyrenes attached onto PGA according to the blob model. The derivation of eq 2 was carried out in an earlier paper[3] using Tachiya's mathematical treatment.[9b]

$$[Py^*]_{(t)} = f \exp\left[-\left(A_2 + \frac{1}{\tau_M}\right)t - A_3(1 - \exp(-A_4 t))\right] + (1 - f)\exp(-t/\tau_M) \quad (2)$$

The parameters A_2, A_3, and A_4 are described in eq 3.

$$A_2 = \langle n \rangle \frac{k_{blob} k_e[blob]}{k_{blob} + k_e[blob]} \qquad A_3 = \langle n \rangle \frac{{k_{blob}}^2}{(k_{blob} + k_e[blob])^2}$$
$$A_4 = k_{blob} + k_e[blob] \quad (3)$$

The time-dependent behavior of the excited pyrene monomers given by eq 2 uses the parameter f which refers to the fraction of pyrene monomers that form excimer by diffusion. The fraction (1 -f) refers to the pyrenes that do not form excimer and fluoresce with their natural lifetime τ_M. The definition of the parameters k_{blob}, k_e[blob], and $\langle n \rangle$ has been given in the Introduction section. The Marquardt−Levenberg algorithm is applied to retrieve the parameters A_2, A_3, and A_4 from the fit of the fluorescence decays. The excimer fluorescence decays were fitted with eq 4 and optimized as discussed in earlier publications.[4,6,7] For all fluorescence decays, the fit was considered good if the χ^2 parameter was less than 1.30 and if the residuals and the autocorrelation function of the residuals were randomly distributed around zero.

$$[E^*] = -[{Py_{diff}}^*]_{(t=0)} e^{-A_3} \sum_{i=0}^{\infty} \frac{{A_3}^i}{i!} \frac{\frac{1}{\tau_M} + A_2 + iA_4}{\frac{1}{\tau_M} - \frac{1}{\tau_{E0}} + A_2 + iA_4} \exp\left(-\left(\frac{1}{\tau_M} + A_2 + iA_4\right)t\right)$$
$$+ \left([E0^*]_{(t=0)} + [{Py_{diff}}^*]_{(t=0)} e^{-A_3} \sum_{i=0}^{\infty} \frac{{A_3}^i}{i!} \frac{\frac{1}{\tau_M} + A_2 + iA_4}{\frac{1}{\tau_M} - \frac{1}{\tau_{E0}} + A_2 + iA_4} \right) e^{-t/\tau_{E0}}$$
$$+ [D^*]_{(t=0)} e^{-t/\tau_D} \quad (4)$$

In eq 4, $[Py_{diff^*}]_{(t=0)}$, $[E0^*]_{(t=0)}$, and $[D^*]_{(t=0)}$ represent the equilibrium concentrations of the pyrenes which form excimer via diffusion, are preassociated and form an excimer upon direct excitation, and are preassociated and form a long-lived excimer upon absorption of a photon, respectively.

Circular Dichroism. Circular dichroism experiments were carried out on a Jasco J-715 spectropolarimeter with UV cells having path lengths of 0.02 and 1.00 cm for studying PyPGA solutions in DMF having pyrene concentrations of 2×10^{-3} and 4×10^{-5} M, respectively. Ten scans were acquired from 250 to 400 nm and averaged. The integral of the ellipticity of the ^1B_b band of pyrene was calculated from 276 to 280.5 nm.

(18) Press: W. H.; Flannery, B. P.; Teukolsky, S. A.; Vetterling, W. T. *Numerical Recipes. The Art of Scientific Computing (Fortran Version)*; Cambridge University Press: Cambridge, 1992; pp 523−528.

Results

Eleven polymers were prepared by random labeling of PGA with 1-pyrenemethylamine. The hydrophobe content of the polymers was described by either the percentage of monomers carrying the pyrene group (expressed in mol %) or the number of moles of pyrene per gram of polymer (λ). The pyrene content ranged from 0.4 to 11.8 mol % and is listed in Table 1. The pyrene-labeled polymers were studied in DMF and in 0.01 M carbonate buffer solutions with 0.05 M NaCl at pH 9, where the backbone adopts a helical[14] and random coil[12] configuration, respectively. Absorbance spectra of the polymer solutions were utilized to qualitatively characterize the association of pyrenes or lack there of. A broadening of the absorption bands is usually observed when pyrene association is present.[16] The peak-to-valley intensity ratio (P_A) provides a measure of this broadness. With pyrenes substituted in the 1-position, a P_A value of 3.0 indicates absence of preassociation. The P_A value decreases with increasing associations.[16] The P_A value equaled 2.5 ± 0.1 for all PyPGAs in DMF. This value is significantly lower than the 2.8 to 2.9 values observed for pyrene-labeled PDMAAms in DMF.[4] The lower than expected P_A values obtained with PyPGA in DMF indicate that some aggregation of the pyrene groups takes place in DMF. In buffer solutions, the P_A value decreased steadily from 2.1 to 1.1 (cf. Table 1) with increasing pyrene content of the polymer. Consequently, more pyrenes are associated in the aqueous buffer solution than in DMF. Furthermore, since the P_A value obtained in aqueous buffer solution decreases with increasing pyrene content, more pyrenes are associated when the pyrene content of the polymer increases.

Steady-state fluorescence spectra were recorded for all PyPGA polymer solutions in both DMF and buffer. In the alkaline buffer solution, the glutamic acid units of PyPGA are ionized and exist as the sodium salt, which is referred to as PyPGNa. Fluorescence measurements were all performed at low polymer concentrations and consequently low pyrene concentrations to prevent intermolecular pyrene excimer formation. The pyrene concentration of all polymer solutions was determined by absorption measurements and was close to $3(\pm 0.3) \times 10^{-6}$ M. In this low concentration range, excimer formation is intramolecular and is not sensitive to slight changes in concentration. Figure 1A shows the spectra of the PyPGA samples in DMF normalized at the 0−0 peak (374 nm). More excimer is being formed intramolecularly as the pyrene content of the polymer increases. Similar trends were obtained in the buffer solutions, however with greater amounts of excimer.

In cases where excimer formation is diffusion-controlled, the solvent viscosity (η(water, 25 °C) = 0.89 mPa·s, η(DMF, 25 °C) = 0.79 mPa·s) is taken into account by multiplying the ratio I_E/I_M by the solvent viscosity. The product of $\eta \times I_E/I_M$ is plotted as a function of pyrene content in Figure 1B. The Birks' scheme predicts a linear increase of the ratio $\eta I_E/I_M$ with concentration for solutions of molecularly separated pyrene.[8] However, for all the polymer samples studied here, whether they are in a random-coil or α-helical conformation, the quantity $\eta I_E/I_M$ increases exponentially with pyrene content in both DMF

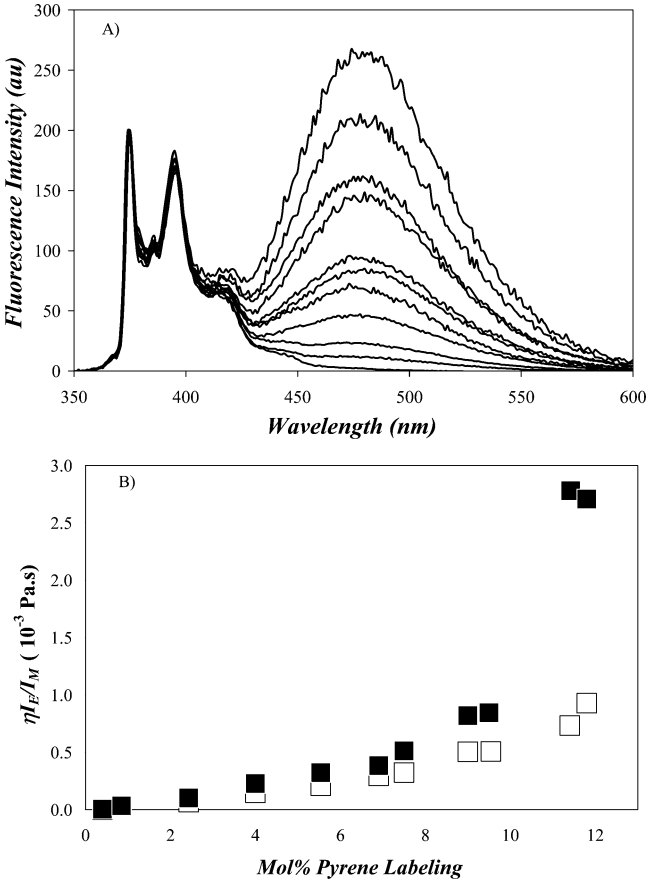

Figure 1. (A) (top) Steady-state fluorescence spectra of PyPGA in DMF normalized at 374 nm. The samples were excited at 344 nm. The excimer peak centered near 490 nm increases with increasing pyrene content in the polymer, λ (μmol·g^{-1}). The pyrene concentration of these polymer solutions was close to 3×10^{-6} M. (B) (bottom) Ratio $\eta I_E/I_M$ as a function of pyrene content, mol % labeling. The pyrene concentration of these polymer solutions was close to 3×10^{-6} M (■ in buffer and □ in DMF).

and aqueous solutions. Similar trends were seen earlier with solutions of polystyrene[3] and poly(*N*,*N*-dimethylacrylamide)[4] that were randomly labeled with pyrene. These differences of behavior are due to the slower dynamics and conformation of the polymer chain which do not ensure a homogeneous distribution of the pyrene pendants throughout the polymer coil. Random labeling of the polymer backbone leads to the creation of pyrene-rich and pyrene-poor regions inside the polymer coil. Whereas this concentration differential would be instantaneously equilibrated for molecular pyrene in homogeneous solutions, this rapid re-distribution of pyrene does not occur in the polymer coil due to constraints imposed by the conformation of the polymer backbone. These considerations apply to PyPGA in DMF even more since the rigid-rod conformation of the backbone is not expected to allow for any rearrangement of the pyrene pendants located along the α-helix.

At least three factors contribute to an enhanced excimer formation. They are the flexibility of the polymer chain, the density of the polymer coil, and the polarity of the solvent. The flexibility of the polymer chain must be considered since a more flexible backbone will facilitate diffusional encounters between pyrenes. The density of the polymer coil also plays a role since a dense conformation will bring pyrenes closer to one another. The polarity of the solvent is important since a more polar solvent (e.g., water) induces the formation of pyrene aggregates

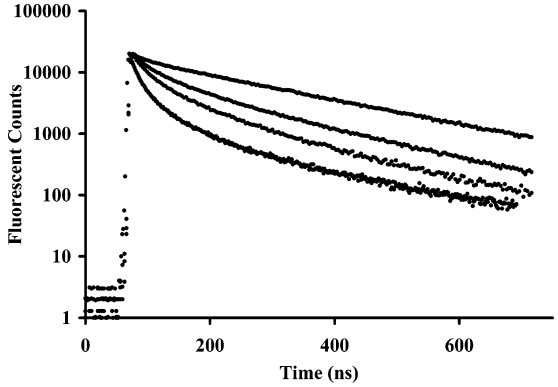

Figure 2. Fluorescence monomer decay profiles for 30-, 300-, 560- and 880-PyPGA in DMF (top to bottom). The samples were excited at 344 nm and emission collected at 375 nm. The pyrene concentration of these polymer solutions was close to 3×10^{-6} M.

which form excimer quasiinstantaneously upon photon absorption. PyPGA in DMF has a rigid backbone and a dense conformation (an α-helix) and thus yields few aggregated pyrenes. PyPGNa in buffer (pH 9) has a relatively rigid backbone and an expanded polymer coil due to same charge electrostatic repulsions of the glutamate ions. These two effects tend to reduce the amount of excimer formed. However, water induces the formation of pyrene aggregates, as shown by the low P_A values obtained for the PyPGNa samples, which is much smaller in aqueous buffer than in DMF (cf. Table 1). The trends shown in Figure 1B where more excimer is formed in water are explained by a more flexible backbone of PyPGNa than PyPGA in DMF and the formation of pyrene aggregates in water.

Fluorescence decay measurements of the pyrene monomer and excimer were carried out on all the polymer solutions in both DMF and buffer solutions. The monomer fluorescence decays obtained in DMF for PyPGA with pyrene contents of 30, 300, 560, and 880 μmol·g^{-1} were normalized at the decay maximum and are shown in Figure 2. Higher pyrene contents lead to greater intramolecular quenching, and the decays exhibit a greater curvature demonstrating faster decay. The results of the multiexponential fit of the monomer decays are listed in Table 2. To obtain a χ^2 smaller than 1.3, two or three exponentials were used to fit the fluorescence decays. The lifetime of the pyrene monomer (τ_M) attached onto the polymer backbone was determined from the fits of the 30-PyPGA decays in DMF and buffer. 30-PyPGA has a very low pyrene content (0.4 mol %) and it forms hardly any excimer as most of the pyrenes exist as single monomers. The fits of the decays of 30-PyPGA in DMF and buffer yielded a long decay time with a contribution of 78% and 93% of the total preexponential weight in DMF and buffer, respectively. Consequently this long decaytime was attributed to τ_M. It was found to equal 215 and 205 ns in DMF and buffer, respectively.

The existence of hydrophobic associations between pyrenes in water, which was determined from the P_A values obtained by UV−vis absorbance measurements, can be confirmed from the analysis of the excimer fluorescence decays. The excimer decays for PyPGA in DMF exhibit a rise time, which is due to the diffusional encounters between pyrenes. No rise time was found for PyPGNa in buffer solutions, indicating that the pyrenes are preassociated, as already confirmed by the P_A values.

Table 2. Parameters Retrieved from the Biexponential or Triexponential Fit of the Pyrene Monomer Fluorescence Decays of PyPGA in DMF and Buffer Solutions (0.01 M Aqueous Carbonate Buffer at pH 9 with 0.05 M NaCl)

solvent	polymer	a_{M1}	a_{M2}	a_{M3}	τ_{M1} (ns)	τ_{M2} (ns)	τ_{M3} (ns)	χ^2
DMF	30-PyPGA		0.22	0.78		29	215	1.23
	70-PyPGA	0.21	0.13	0.66	18	92	215	1.20
	180-PyPGA	0.33	0.34	0.33	36	136	215	1.16
	300-PyPGA	0.46	0.36	0.18	26	101	215	1.23
	420-PyPGA	0.53	0.42	0.05	26	80	215	1.31
	520-PyPGA	0.57	0.32	0.12	26	96	215	1.25
	560-PyPGA	0.60	0.32	0.08	23	87	215	1.33
	670-PyPGA	0.63	0.30	0.06	18	70	215	1.36
	720-PyPGA	0.66	0.28	0.05	15	61	215	1.29
	860-PyPGA	0.66	0.29	0.06	12	49	215	1.18
	880-PyPGA	0.71	0.25	0.04	11	50	215	1.26
buffer	30-PyPGA		0.08	0.92		31	205	1.22
	70-PyPGA	0.09	0.12	0.79	9	91	205	1.02
	180-PyPGA	0.18	0.43	0.39	48	189	205	1.19
	300-PyPGA	0.17	0.32	0.50	26	126	205	1.14
	420-PyPGA	0.26	0.33	0.41	32	130	205	1.02
	520-PyPGA	0.29	0.35	0.36	23	122	205	1.24
	560-PyPGA	0.32	0.45	0.24	29	136	205	1.28
	670-PyPGA	0.48	0.32	0.21	20	110	205	1.30
	720-PyPGA	0.43	0.34	0.23	24	94	205	1.19
	860-PyPGA	0.46	0.34	0.20	18	93	205	1.25
	880-PyPGA	0.51	0.31	0.19	19	97	205	1.25

Table 3. Parameters Retrieved from the Triexponential Fit of the Pyrene Excimer Fluorescence Decays of PyPGA in DMF and Buffer Solutions (0.01 M Aqueous Carbonate Buffer at pH 9 with 0.05 M NaCl)

solvent	polymer	a_{E1}	a_{E2}	a_{E3}	τ_{E1} (ns)	τ_{E2} (ns)	τ_{E3} (ns)	χ^2
	300-PyPGA	−0.61	0.90	0.10	17	67	138	0.99
	420-PyPGA	−0.52	0.90	0.10	15	63	108	1.25
	520-PyPGA	−0.55	0.93	0.07	15	61	128	1.05
	560-PyPGA	−0.54	0.92	0.08	15	63	110	1.18
DMF	670-PyPGA	−0.55	0.90	0.11	13	56	91	1.14
	720-PyPGA	−0.49	0.93	0.07	12	56	100	1.16
	860-PyPGA	−0.50	0.92	0.08	10	53	90	1.12
	880-PyPGA	−0.54	0.88	0.13	10	52	77	1.13
	300-PyPGA	0.24	0.70	0.06	21	45	114	1.01
	420-PyPGA	0.18	0.74	0.09	15	42	101	1.07
	520-PyPGA	0.17	0.71	0.12	11	41	87	1.09
buffer	560-PyPGA	0.19	0.69	0.13	10	40	84	1.22
	670-PyPGA	0.19	0.66	0.16	13	42	82	1.23
	720-PyPGA	0.17	0.62	0.21	17	42	80	0.99
	860-PyPGA	0.14	0.52	0.34	8	40	77	1.12
	880-PyPGA	0.12	0.63	0.25	10	48	88	1.00

All the excimer fluorescence responses were fitted with three exponentials (cf. Table 3). Six parameters were obtained from the fitting, namely, the rise time (τ_{E1}), two decay times (τ_{E2} and τ_{E3}), and their corresponding preexponential weights (a_{E1}, a_{E2}, and a_{E3}). In the presence of a rise time, the amplitude a_{E1} is negative. If one calls ξ the ratio $a_{E1}/(a_{E2} + a_{E3})$, ξ equals -1.0 when no preassociated pyrenes are present and excimers are formed via diffusional encounters of pyrenes only. The ratio ξ is expected to equal 0.0 when all the pyrenes are in a preassociated form. In the buffer solutions, this value is actually larger than 0.0 (0.21 ± 0.05 for PyPGNa with pyrene contents ranging from 300 to 880 μmol·g^{-1}), due certainly to complications arising from having pyrenes so close to one another inside the pyrene aggregates. To form an excimer, two pyrenes must stack with a well-defined geometry corresponding to the energy minimum resulting from the interaction between an excited pyrene monomer and a ground-state pyrene monomer. In a pyrene aggregate in water, the pyrenes arrange themselves in a manner which will minimize the solvation energy of the pyrene aggregate. Because the energy requirements to form a pyrene excimer are different from that of forming a pyrene aggregate, direct excitation of a pyrene aggregate might not always result in the formation of an excimer but of a hybrid species. This might explain the existence of long-lived pyrene excimers which has been already reported by this laboratory[4−7] and others.[19] This long-lived excimer is taken into account for the analysis of the excimer fluorescence decays by introducing the species denoted by D in eq 4, as done in earlier studies.[4,6,7] However, its existence does not explain the positive ξ values, which are due to the positive value taken by the preexponential factor a_{E1} associated with the short decay time τ_{E1}. This fast decay time indicates that a fast process occurs at the early times. This fast process could be energy hopping which is known to take place in domains densely packed with chromophores such as pyrene aggregates.

The ratio ξ was found to equal -0.53 ± 0.05 in DMF for polymers with pyrene contents ranging from 300 to 880 μmol·g^{-1}. The polymers with lower pyrene content ($\lambda < 300$ μmol·g^{-1}) yielded much less excimer, disallowing a reasonable acquisition time of the excimer decays with our instrument; their decays were not acquired. The ξ value of -0.53 ± 0.05 for PyPGA in DMF is more positive than the one found for the pyrene labeled poly(*N*,*N*-dimethylacrylamide) (PyPDMAAm) in acetone or DMF (-0.75 ± 0.07).[4] This indicates that more ground-state pyrenes are present in PyPGA than in PyPDMAAm in DMF, a conclusion in agreement with the P_A values found by UV−vis absorbance. To this date, the ideal ξ value of -1.0 has never been found for excimers formed between pyrenes randomly attached onto a polymer backbone. This is believed to be due to the random incorporation of pyrenes at neighboring positions that form excimer on a fast time scale, making them indistinguishable from excimers formed via direct excitation of pyrenes preassociated inside a pyrene aggregate. The ξ and P_A values indicate that pyrene is incorporated in a more clustered manner in PyPGA than expected. Two reasons can be invoked to rationalize this result. The first one involves the procedure used to synthesize the pyrene-labeled polymers. 1-Pyrenemethylamine did not fully dissolve in the reaction mixture, and cloudy suspensions were observed. This could have led to the successive incorporation of pyrenes along the backbone. The second reason involves the coil-to-helix transition, which occurs when PGA is removed from the reaction mixture, where it is present in its ionic form as a random coil, and placed in DMF, where it has been re-acidified into the helical polyacid form. Even if pyrenes are attached randomly at non-neighboring positions onto PGNa during the pyrene labeling procedure, they may find themselves in close proximity when the polymer is dissolved in DMF in its re-acidified form, where it adopts the denser α-helical conformation. Since there are 3.6 residues per turn of the α-helix, one can imagine that two pyrenes attached on two glutamic acids separated by two other residues can end up at neighboring positions in the α-helix.

To obtain quantitative information on the dynamics of pyrene encounters and the fraction of associated pendants, the blob model was utilized. For a polymer in a random-coil conforma-

(19) (a) Piçara, S.; Gomes, P. T.; Martinho, J. M. G. *Macromolecules* **2000**, *33*, 3947−3950. (b) Reynders, P.; Dreeskamp, H.; Kühnle, W.; Zachariasse, K. A. *J. Phys. Chem.* **1987**, *91*, 3982−3992. (c) Pandey, S.; Kane, M. A.; Baker, G. A.; Bright, F. V.; Fürstner, A.; Seidel, G.; Leitner, W. *J. Phys. Chem. B* **2002**, *106*, 1820−1832.

Table 4. Parameters Retrieved from the Blob Model Analysis of the Pyrene Monomer Fluorescence Decays of PyPGA in DMF and Buffer Solutions (0.01 M Aqueous Carbonate Buffer at pH 9 with 0.05 M NaCl), According to Equation 2

solvent	polymer	f	k_{blob} (10^7 s^{-1})	$\langle n \rangle$	k_e[blob] (10^7 s^{-1})	χ^2
	30-PyPGA	0.30				
	70-PyPGA	0.35				
	180-PyPGA	0.64	1.4	1.11	0.4	1.04
	300-PyPGA	0.81	1.7	1.46	0.5	1.07
	420-PyPGA	0.95	1.5	1.77	0.7	1.16
DMF	520-PyPGA	0.89	1.8	1.73	0.4	1.16
	560-PyPGA	0.92	1.7	1.87	0.4	1.17
	670-PyPGA	0.94	2.1	2.05	0.6	1.19
	720-PyPGA	0.95	2.7	2.12	0.7	1.06
	860-PyPGA	0.93	2.5	2.26	0.7	1.15
	880-PyPGA	0.94	2.8	2.38	0.6	1.08
	30-PyPGA	0.09				
	70-PyPGA	0.28				
	180-PyPGA	0.28				
	300-PyPGA	0.48	2.7	0.68	0.7	1.13
	420-PyPGA	0.57	1.7	0.96	0.5	1.04
buffer	520-PyPGA	0.61	3.2	0.90	0.6	1.21
	560-PyPGA	0.70	2.4	0.82	0.5	1.09
	670-PyPGA	0.79	2.7	1.30	0.4	1.10
	720-PyPGA	0.77	1.8	1.47	0.4	1.11
	860-PyPGA	0.81	3.0	1.31	0.6	1.15
	880-PyPGA	0.79	3.2	1.43	0.6	1.28

tion, a blob is defined as the volume probed by an excited pyrene while it remains in the excited state.[3−7] By analogy, a blob for a PGA α-helix will be that section of the helix which can be probed by an excited pyrene located at the tip of a glutamic acid side chain. Consequently, the blob model is expected to apply whether PGA adopts an α-helical conformation in DMF or is a random coil in aqueous buffer solutions at pH 9. All monomer decays were fitted well with eq 2. The retrieved parameters f, k_{blob}, $\langle n \rangle$, and k_e[blob] are listed in Table 4 and summarized in Table 5. The fraction f denotes the fraction of pyrenes forming excimer via diffusion, a process handled by the blob model analysis. The parameters retrieved from the blob model analysis are examined as a function of the corrected pyrene content λ/f. In all of the pyrene-labeled polymers studied so far, the fraction of pyrenes forming excimer via diffusion (f) was close to 1.0. This is not the case for PyPGNa where f remains substantially smaller than 1.0 in water and tends to 1.0 for PyPGA samples in DMF having pyrene contents larger than 300 μmol·g^{-1}. Consequently, a significant portion of the monomer decays is described by the second exponential in eq 2, which represents the emission of isolated pyrenes. Less information is available in the decays for the fit of the first exponential of eq 2 to yield highly accurate A_2, A_3, and A_4 values. As a result, the parameters retrieved from the blob model analysis of the PyPGA and PyPGNa decays are more scattered than those presented in earlier studies.[3−5]

The size of the blob in terms of the number of monomer units was determined from the average number of quencher per blob $\langle n \rangle$ using eq 5.[3−5] In eq 5, x is the mole fraction of glutamic

$$N_{blob} = \frac{\langle n \rangle}{(\lambda/f)(358x + 145(1 - x))} \tag{5}$$

acids modified with 1-pyrenemethylamine. The values 358 and 145 expressed in g·mol^{-1} represent the molar masses of the pyrene-labeled glutamic acid and unlabeled glutamic acid. N_{blob} is plotted as a function of the corrected pyrene content in Figure 3. The N_{blob} value must be considered with caution when pyrene aggregates are present in solution. As argued in previous reports,[4,6,7] a pyrene aggregate acts as a single quencher so that the number of quencher per blob, $\langle n \rangle$, might be smaller than the actual number of pyrene per blob if pyrene aggregates are present. Consequently, eq 5, which assumes that each pyrene acts as a quencher, will yield lower N_{blob} values if pyrene aggregates are present in solution. To assess the validity of the N_{blob} values retrieved from the blob model analysis, it is necessary to determine the level of pyrene association to establish the conditions when the pyrene ⇔ quencher equivalence holds. The determination of the level of pyrene aggregation is done by applying a procedure established in two earlier reports.[4,7] This procedure is summarized in the following paragraph.

Although ξ and P_A provide qualitative information about the presence of pyrene aggregates, quantitative information about the amount of aggregation is obtained by determining the parameters f_{diff}, f_{free}, f_{E0}, and f_D whose definitions are given in eq 6a−d. The parameters f_{diff}, f_{free}, f_{E0}, and f_D represent the fractions of pyrene monomers which form excimer via diffusion (Py_{diff}^*), are isolated and do not form any excimer (Py_{free^*}), are involved in a pyrene aggregate which forms an excimer upon direct excitation (E0*), and are involved in a pyrene aggregate which forms a long-lived excimer (D*), respectively. These parameters are retrieved by applying the blob model analysis to the monomer and excimer fluorescence decays. Analysis of the monomer decays yields the fractions of pyrenes which are either isolated or form excimer via diffusion (cf. eq 2). Analysis of the excimer decays yields the fraction of pyrenes which form excimer via either diffusion or direct excitation of associated ground-state pyrenes (cf. eq 4). The important step in the analysis consists of "matching" the fraction of pyrenes forming excimer via diffusion obtained from the monomer and excimer decay analyses.[4,7] The level of association f_{agg} was determined in DMF by this methodology. In buffer, f_{agg} was assumed to be close to its maximum value of 1.0. This is because in buffer the pyrene excimer is formed overwhelmingly via the direct excitation of associated ground-state pyrenes and the excimer decays did not yield the fraction of pyrenes forming excimer by diffusion.

$$f_{diff} = \frac{[Py_{diff}^*]_{(t=0)}}{[Py_{diff}^*]_{(t=0)} + [Py_{free}^*]_{(t=0)} + [E0^*]_{(t=0)} + [D^*]_{(t=0)}} \tag{6a}$$

$$f_{free} = \frac{[Py_{free}^*]_{(t=0)}}{[Py_{diff}^*]_{(t=0)} + [Py_{free}^*]_{(t=0)} + [E0^*]_{(t=0)} + [D^*]_{(t=0)}} \tag{6b}$$

$$f_{E0} = \frac{[E0^*]_{(t=0)}}{[Py_{diff}^*]_{(t=0)} + [Py_{free}^*]_{(t=0)} + [E0^*]_{(t=0)} + [D^*]_{(t=0)}} \tag{6c}$$

$$f_D = \frac{[D^*]_{(t=0)}}{[Py_{diff}^*]_{(t=0)} + [Py_{free}^*]_{(t=0)} + [E0^*]_{(t=0)} + [D^*]_{(t=0)}} \tag{6d}$$

The excimer decays exhibited a long-lived component, which was observed in the triexponential fits (cf. Table 3). The long

Table 5. Summary of the Parameters Retrieved by the Blob Model Analysis of the Monomer Fluorescence Decays of Py-PGA

solvent	η (mPa·s)	k_{blob} (10^7 s^{-1}) as a function of λ in μmol·g^{-1}	N_{blob} as a function of λ in μmol·g^{-1}	k_e[blob] (10^6 s^{-1})
DMF	0.79	$(2.0 \pm 0.3) \times 10^{-3}\ \lambda/f + (0.8 \pm 0.2)$	$(-2.0 \pm 0.2) \times 10^{-2}\ \lambda/f + (32 \pm 1)$	4 ± 1
buffer	0.89	2.6 ± 0.6	7.9 ± 1.3	5 ± 1

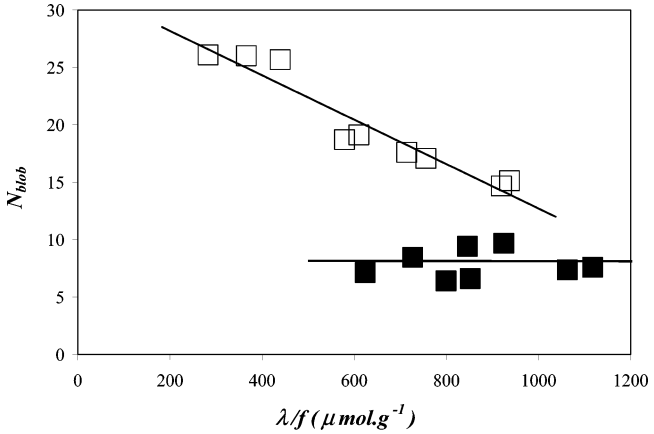

Figure 3. Plot of N_{blob} for PyPGA and PyPGNa polymers as a function of pyrene content (■ in buffer and □ in DMF).

Table 6. Parameters Obtained from Fitting the Excimer Fluorescence Decays with Equation 4 for Py-PDMAAm in DMF (τ_D = 110 ns)

polymer	f_{diff}	f_{free}	f_{E0}	f_D	τ_{E_0}	χ^2
300-PyPGA	0.61	0.14	0.17	0.08	42	1.14
420-PyPGA	0.56	0.03	0.34	0.07	52	1.27
520-PyPGA	0.56	0.07	0.30	0.07	48	1.20
560-PyPGA	0.57	0.05	0.31	0.07	48	1.21
670-PyPGA	0.59	0.04	0.33	0.04	47	1.19
720-PyPGA	0.44	0.02	0.49	0.04	49	0.96
860-PyPGA	0.41	0.03	0.53	0.03	48	1.32
880-PyPGA	0.46	0.03	0.48	0.03	47	1.15

decay time (τ_{E2}) equaled 108 ± 21 ns in DMF. As typically done in earlier studies,[4,6,7] τ_{E3} retrieved from the triexponential fits was arbitrarily equated to the lifetime of the long-lived excited dimers τ_D and fixed to equal 110 ns in the evaluation of the excimer decays with eq 4. The values of the parameters f_{diff}, f_{free}, f_{E0}, f_D, τ_{E0}, and χ^2 are listed in Table 6. The fits for the excimer fluorescence decays were found to be good in all cases (cf. χ^2<1.3). The excimer lifetime, τ_{E0}, determined from the analysis of the excimer decays was found to equal 47±3 ns, a reasonable value for the lifetime of the pyrene excimer.[4−8] The fraction of aggregated pyrene pendants (f_{agg}) is given by the sum of f_{E0} and f_D. It is plotted as a function of μ/f in Figure 4. The parameter μ is the number of pyrenes per backbone atom. It is expressed in mol %.

The f_{agg} values shown in Figure 4 for PyPGA in DMF are between 0.20 and 0.55. This behavior is different from that observed with PyPDMAAms for which f_{agg} was always smaller than 0.20.[4] As argued earlier, the large f_{agg} values for PyPGA can be a consequence of solubility issues encountered during the labeling procedure and the coil versus helix conformation of PGA and PGNa present in buffer and DMF solutions, respectively. As the pyrene content decreases, the fraction of preassociated pyrenes decreases as well, indicating that the pyrenes are more isolated at low pyrene contents and spread more evenly along the α-helix.

The conclusion that the fraction of clustered pyrenes increased as a function of pyrene content was confirmed by carrying out

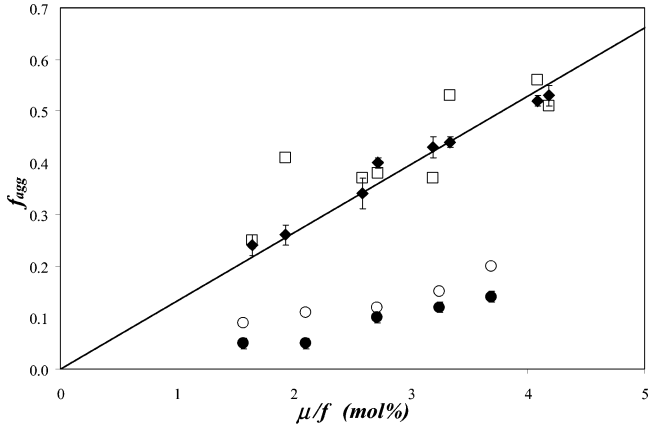

Figure 4. Fraction of associated pyrenes (f_{agg}) as a function of the corrected pyrene content, μ/f (mol %), for PyPGA (□) and PyPDMAAm (○, from ref 4) studied in DMF and f_{agg} values obtained from simulations assuming that pyrenes are randomly distributed along an α-helix (◆) or a linear chain (●).

circular dichroism (CD) experiments in DMF. CD has been used successfully to quantify the orientation of pyrene pendants of 25, 45, and 100 mol % labeled PyPGA in *N*,*N*-dimethylacetamide (DMAC).[15] In these studies, the CD signal is reported to arise from exciton coupling of positive exciton chirality. Although the 1-pyrenemethylene side group is not optically active, the fact that it is a bulky chromophore and is connected to the PGA α-helix via a rigid amide linkage induces exciton chirality in the side chains. According to this earlier study, CD experiments were expected to probe exciton coupling arising from those pyrenes clustered along our PyPGA samples. CD spectra were acquired for PyPGA solutions in DMF with pyrene concentrations of 2×10^{-3} and 4×10^{-5} M at wavelengths larger than 250 nm, since DMF absorbs strongly at shorter wavelengths. The trends obtained at both concentrations were the same, and Figure 5 shows the spectra acquired for the concentration of 2×10^{-3} M. The ellipticity values, [θ], were low, reflecting the low pyrene content of the PyPGA samples and the freedom experienced by the isolated pyrenes. The low [θ] values led to higher noise levels in the CD spectra shown in Figure 5A when compared to those obtained with PyPGA in DMAC containing higher levels of pyrene labeling.[15] The overall shape of the spectra however agreed well with those reported for 25, 45, and 100 mol % labeled PyPGA in DMAC.[15] The CD signal was detected in the ^1L_a (350 nm) and ^1B_b (280 nm) bands of the pyrene chromophore. The ellipticity of the ^1B_b band integrated from 276 to 280.5 nm is plotted in Figure 5B as a function of pyrene content for PyPGA, PyPDMAAm, and the model compound 1-pyrenemethylacrylamide (PyMAAm) in DMF. All PyPGA samples exhibited [θ] values larger than the one obtained for PyMAAm.[20] Figure 5B demonstrates that the [θ] value of PyPGA increases linearly with pyrene content, indicating that the pyrene moieties become more oriented as more pyrene is attached onto the backbone. It agrees with the suggestion that pyrene attaches itself in a clustered manner onto

(20) The synthesis of PyMAAm is reported in an earlier publication.[4]

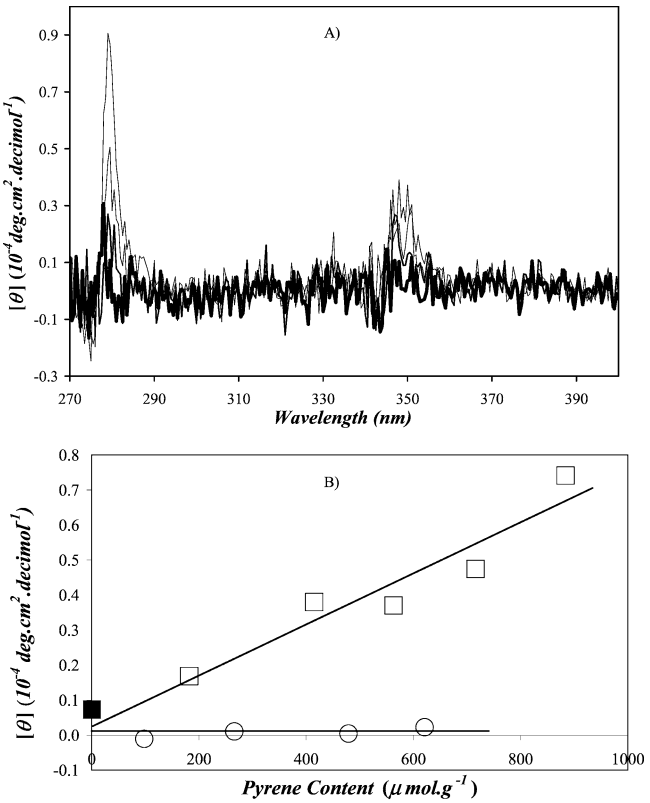

Figure 5. (A) Circular dichroism spectra with a pyrene concentration of 2×10^{-3} M in DMF carried out in a 0.02 cm cell. From top to bottom: 880-PyPGA, 560-PyPGA, 180-PyPGA, and PyMAAm (thick line). (B) Average ellipticity values for (□) PyPGA, (■) PyMAAm, and (○) PyPDMAAm samples in DMF.

PGA, as inferred from the large f_{agg} and more positive ξ values obtained with our fluorescence measurements and the lower P_A values obtained by UV−vis absorption. The ellipticity of PyPGA in DMF at 280 nm intercepts the *Y*-axis at a value very close to the ellipticity of the unoriented PyMAAm model compound. The $[\theta]$ value of PyMAAm was taken as the $[\theta]$ value of a PGA sample having an infinitesimally small pyrene content for which each pyrene would have a random orientation along the α-helix.

CD spectra were also acquired for PyPDMAAm[4,5] at the same pyrene concentration. Since PDMAAm adopts a random coil conformation in DMF, no CD signal was obtained for PyPDMAAm, despite the fact that 1-pyrenemethylamine is covalently linked onto PDMAAm via the same rigid amide bond used to label PGA with pyrene and that the linker separating the pyrene moiety from the polymer backbone is made of three and five atoms for pyrene labeled PDMAAm and PGA, respectively. With pyrene being located closer to the PDMAAm backbone, the pyrene attached onto the PDMAAm backbone would be expected to exhibit a greater orientation which should be reflected by $[\theta]$ values being larger than for the PGA samples. The opposite is observed. The PyPGA samples exhibit larger $[\theta]$ values than PyPDMAAm demonstrating that the pyrene moieties of PyPGA attached in a clustered manner onto a polymer adopting an α-helical conformation in DMF.

To demonstrate that the compact structure of the PGA α-helix could yield the large f_{agg} values shown in Figure 4, simulations were carried out. A string of 300 units (comparable in size to the PGA sample under study) was generated and a fraction of these units was randomly selected (i.e., labeled with pyrene) using the random number generator RAN1.[18] The geometry of the α-helix implies that a pendant located at position 0 will be next to a second pendant if the second pendant is located at positions −4, −3, −1, and +1, +3, +4. The program determined the fraction of the pendants which were not close to another pendant equivalent to the sum $f_{free} + f_{diff}$ (cf. eqs 6a,b). Taking $1 - (f_{free} + f_{diff})$ yielded f_{agg}. Forty such simulations were performed, and the averages and standard deviations were calculated. They are presented in Figure 4. The agreement with the experimental results is very good. Not only do these simulations confirm the unavoidable clustering of the pyrene pendants induced by the geometry of the α-helix but they also provide the first quantitative confirmation of the validity of the blob model approach to determine the fraction of associated pyrenes randomly attached onto a polymer. The simulations were repeated for a linear chain where a neighboring pyrene was assumed to be at position −1 and +1. The parameter f_{agg} dropped to much lower values close to those obtained for PyPDMAAm samples in DMF (cf. Figure 4). However the simulated f_{agg} values are slightly lower than those obtained experimentally for PyPDMAAm. This is due to the fact that the units making up PDMAAm contribute two atoms to the backbone, whereas a PGA unit contributes three atoms to the backbone. The perfect match observed for the f_{agg} values obtained experimentally and by simulations for PyPGA in DMF suggests that a pyrene molecule covers three backbone atoms and is expected to reach farther than the two backbone atoms of a *N*,*N*-dimethylacrylamide unit. Consequently, the simulations, which do not identify the number of backbone atoms of a monomer, yield underestimated f_{agg} values for PyPDMAAm.

Fluorescence excitation spectra were also acquired because the observation of a shift between the excitation of the pyrene monomer, obtained at an emission wavelength (λ_{em}) of 376 nm, and the excimer, obtained at λ_{em} of 500 nm, is an indication of the presence of ground-state pyrene dimers. Typical excitation spectra of PyPDMAAm in DMF, PyPGA in DMF, and PyPGNa in buffer are given in Figure 6. No shift is observed for the polymer samples dissolved in DMF, but a clear alteration of the excimer fluorescence excitation spectrum is observed in Figure 6C), which demonstrates the presence of ground-state pyrene aggregates in aqueous solution. The nice overlap of the excitation spectra of PyPGA in DMF might appear at odd with our claim that pyrenes are clustered on the PGA backbone in DMF. However, it is important to consider that, although all PyPGA samples in DMF exhibit some pyrene aggregation, the fraction of pyrenes forming excimer by diffusion remains large and ranges from 41 up to 61 mol % (cf. Table 6). It seems that the large number of pyrenes forming excimer by diffusion are enough to ensure that the excitation spectra of the pyrene monomer and excimer overlap for PyPGA in DMF. These results are actually very similar to those presented by Pandey et al.[19c] They report that the excimer decay acquired in acetonitrile for an 18 atom long chain end-labeled with two pyrenes exhibits a ξ value of −0.70, which indicates the presence of ground-state pyrene dimers, although the excitation spectra of the pyrene monomer and excimer overlap. These results imply that the presence of pyrene aggregates cannot always be inferred from the shift of the excitation spectra. From

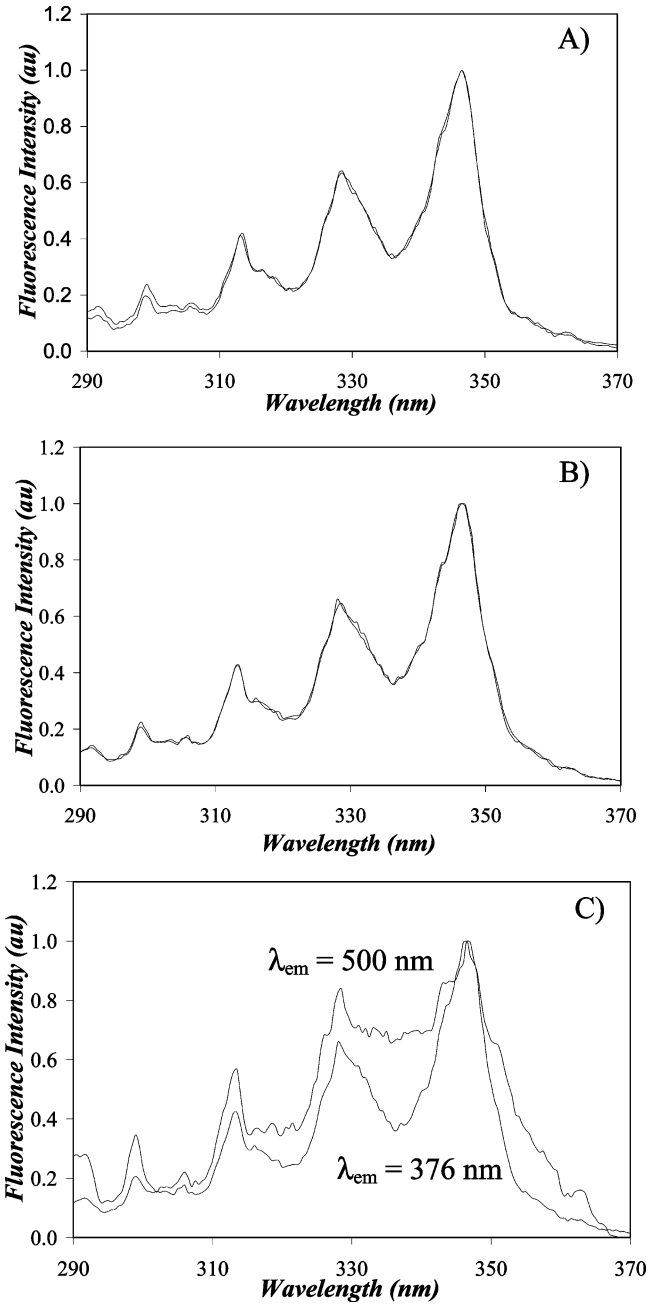

Figure 6. Fluorescence excitation spectra acquired at λ_{em}(monomer) = 376 nm and λ_{em}(excimer) = 500 nm for (A) PyPDMAAm (7.3 mol % of pyrene) in DMF, (B) PyPGA (5.5 mol % of Py) in DMF, and (C) PyPGNa (5.5 mol % of Py) in carbonate buffer at pH 9.

this study, it appears that a careful analysis of the excimer decay is more sensitive to the presence of ground-state pyrene dimers.

The trends shown in Figures 4 as obtained from the analysis of the fluorescence monomer and excimer decays and 5 from CD both indicate that the amount of clustered pyrenes increases with pyrene content. The increase in pyrene aggregation with pyrene content yields underestimated $\langle n \rangle$ values which explains the decrease of N_{blob} with pyrene content observed in Figure 3 (cf. eq 5). However, the level of pyrene clustering decreases with decreasing pyrene content. Consequently, the pyrene ⇔ quencher equivalence is expected to hold for lower pyrene contents. The N_{blob} value for PyPGA in DMF was determined by extrapolating the N_{blob} values shown in Figure 3 to zero pyrene content. In doing so, N_{blob} was estimated to equal 32 ± 1 for PGA in DMF.

Discussion

At this stage of the study, several points have been established about the PyPGA system in DMF. The peak-to-valley ratios P_A obtained by UV−vis absorption (cf. Table 1), the ratios of the preexponential factors ξ obtained from the triexponential fit of the excimer decays (cf. Table 3), the levels of association f_{agg} obtained with the blob model analysis (cf. Figure 4), and the ellipticity values obtained by CD (cf. Figure 5) all demonstrate that pyrene is attached onto the PGA backbone in a clustered manner. In these experiments, the P_A and ξ values result from the combined response of the pyrene monomers and aggregates. The P_A value reflects the overlap between the absorption of the pyrene monomers and the pyrene aggregates whereas the kinetics of excimer formation predict that the preexponential factors used to determine the parameter ξ are a complicated combination of the concentrations of the pyrene monomer and excimer (cf. eq 4). On the other hand, the ellipticity value, which results from exciton coupling between nearby pyrenes (i.e., aggregated pyrenes), and the f_{agg} parameter are a direct measure of the concentration of aggregated pyrenes. Both parameters indicate that the level of clustering decreases at low pyrene content so that information about the unlabeled PGA polymer can be obtained by plotting the different parameters (k_{blob} and N_{blob}) as a function of pyrene content and extrapolating the trends to zero pyrene content. Using this extrapolation method, the results for α-helical PGA in DMF (the α-helical conformation was demonstrated in an earlier study and is supported by our CD results) are compared to those obtained with the random coil PyPDMAAm.[4,5] In the case of PyPGA in DMF, excimer formation reflects the encounters between pyrenes attached onto the rigid α-helical PGA backbone via a flexible tether, whereas excimer formation in the case of PyPDMAAm reflects the long-range dynamics of the PDMAAm random coil. The data obtained in alkaline buffer are not considered due to the very high level of aggregation (f_{agg} ∼1.0).

The rate constant k_{blob} is inversely proportional to the blob volume.[3−7] This comes from the very definition of k_{blob} which is the rate constant for the encounters taking place between one excited pyrene and one ground-state pyrene located in the same blob containing these two pyrenes only. A plot of k_{blob} versus μ/f is shown in Figure 7. The parameter μ is the number of pyrenes per backbone atom. It is expressed in mol %. For PyPGA in DMF, k_{blob} increases with pyrene content, indicating that the volume of the blob decreases with pyrene content. This result is internally consistent with the trend shown in Figure 3, where N_{blob} is shown to decrease with pyrene content. An extrapolation of k_{blob} to the *Y*-axis yields the k_{blob} value of an ideal PyPGA sample where the pyrene groups are evenly distributed along the α-helix (no pyrene aggregates are present). The value of k_{blob} extrapolated for a μ value of 0 μmol·g^{-1} equals 0.8(±0.2) × 10^7 s^{-1} for PGA in DMF. It is close to the k_{blob} value of 1.1(±0.1) × 10^7 s^{-1} obtained for PDMAAm in DMF.[4] The similarity of the k_{blob} values obtained for the α-helical PGA and the random coil PDMAAm in DMF can be explained in the following manner. The value of k_{blob} is expected to increase if the backbone is more flexible and the polymer coil adopts a more compact conformation.

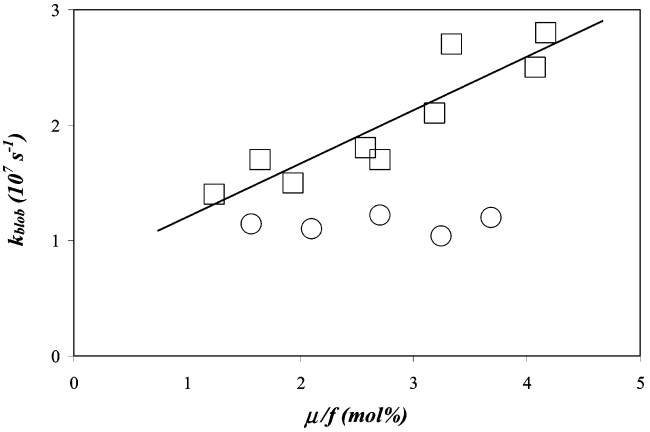

Figure 7. Parameter k_{blob} as a function of the number of pyrene per backbone atom (μ expressed in mol %) divided by the fraction f obtained from fitting the monomer decays by eq 2. (□) PyPGA and (○) PyPDMAAm samples in DMF.

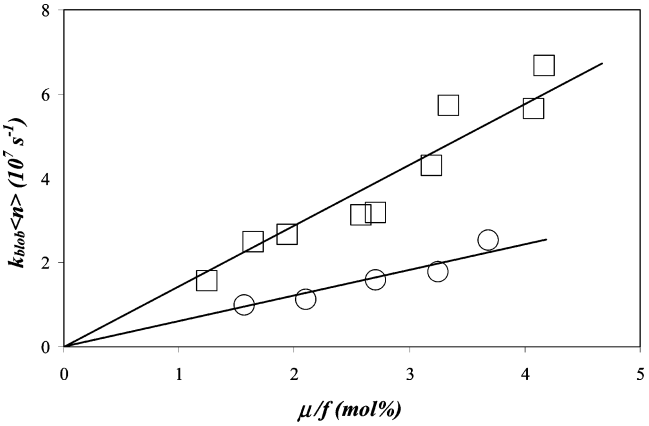

Figure 8. Product $k_{blob}\langle n\rangle$ as a function of the number of pyrene per backbone atom (μ expressed in mol %) divided by the fraction f obtained from fitting the monomer decays by eq 2. (□) PyPGA and (○) PyPDMAAm samples in DMF.

In the case of the α-helical PGA, the backbone is rigid and the conformation of the polymer is very compact. On the other hand, the backbone of PDMAAm is flexible, but its polymer coil is expanded since DMF has been shown to be a good solvent for PDMAAm.[4,5] Consequently, both effects counteract one another to yield similar k_{blob} values for PGA and PDMAAm in DMF.

Throughout this Article, PGA in DMF is described as being a rigid rod. The description of a polymer as being rigid is a qualitative statement which can be made more quantitative by using the persistence length of the polymer. It is the length over which the chain persists in the same direction as the first bond. Polyolefins usually have persistence lengths smaller than 2 nm.[21] In comparison, α-helices in organic solvents have been found to exhibit persistence lengths larger than 50 nm.[22] Consequently, α-helices can be qualified as being much more rigid than polyolefins. Since the length of an α-helix increases by 0.15 nm per amino acid, a PGA blob in DMF made of 32 amino acids is 4.8 nm long and can be considered as a rigid rod, because its length is at least 10 times shorter than the PGA persistence length. Consequently excimer formation between two pyrenes is the result of the motion of the PGA side chains which allow the pyrene groups to encounter around the rigid PGA α-helix.

A PGA blob in DMF is made of 32 ± 1 amino acids. By definition, the parameter k_{blob} represents the rate constant at which two pyrenes encounter when they are located inside the same blob. A PGA blob with two pyrenes can be visualized as having one pyrene at the center of a section of the PGA α-helix flanked by two stretches of 15 ± 1 glutamic acids on both sides onto which the second pyrene moiety can attach itself. The pyrene moieties attached at the end of two glutamic acid side chains encounter with a rate constant of $0.8(\pm 0.2) \times 10^7$ s^{-1}. A PGA blob, being much shorter than the persistence length of an α-helix, can be considered as being a rigid rod. Thus the pyrene encounters are controlled by the dynamics of the PGA side chains, and the blob model, via the k_{blob} parameter, provides information about the rate at which PGA side chains probe the space surrounding them.

Since the pseudo-unimolecular rate constant k_{blob} is inversely proportional to the volume of a blob and the parameter $\langle n\rangle$ represents the average number of quenchers per blob, the product $k_{blob}\langle n\rangle$ is proportional to the local concentration of quencher inside the polymer coil.[3−5] This is indeed observed in Figure 8 where the product $k_{blob}\langle n\rangle$ is plotted as a function of μ/f. The slope of the straight line obtained for PyPGA in DMF is 2.4 times steeper than that obtained for PyPDMAAm in DMF, which indicates that the density of backbone atoms of PyPGA in DMF is at least 2.4 times larger than that of PyPDMAAm in DMF. This is a reasonable conclusion since the α-helical PGA is expected to be denser than the PDMAAm random coil. The value of 2.4 represents only the lower limit for the density of backbone atoms due to the presence of the pyrene aggregates which leads to reduced $\langle n\rangle$ values and, in turn, an underestimated $k_{blob}\langle n\rangle$ product.

The blob model predicts that a PGA-blob is made of 32 ± 1 units. To establish that the blob model can be applied to the study of polypeptides exhibiting secondary structure, it is important to determine whether an N_{blob} value of 32 ± 1 is compatible with the geometry of a system, where pyrene groups are randomly attached along an α-helix. Since two pyrenes located inside the same blob form an excimer with the rate constant k_{blob}, the blob model implies that two pyrenes can overlap and form an excimer when they are located inside a 32 amino acid (a.a.) section of the α-helix. The symmetry of the α−helix imposes that if a pyrene moiety is located at the center of the blob (i.e., on the 16th residue), an excimer will be formed if a second pyrene located within 16 residues of the first pyrene and on either side of the first pyrene can exhibit some overlap with the first one. Molecular mechanics optimizations were carried out in order to determine the minimum number of residues which must be introduced between two pyrenes located along a PGA α-helix to prevent any overlap.

An α-helix made of 32 glutamic acids was generated with the program Hyperchem (release 7.02 for Windows). A first

(21) Yoon, D. Y.; Flory, P. J. *J. Polym. Sci.*: *Polym. Phys. Ed.* **1976**, *14*, 1425−1431.
(22) Wada, A.; Kihara, H. *Polym. J.* **1972**, *3*, 482−487. Moha, P.; Weill, G.; Benoit, H. *J. Chem. Phys.* **1964**, *61*, 1240−4.
(23) Stryer, L. *Biochemistry*, 4th ed.; W. H. Feeman and Company: New York, 1995; p 418.
(24) Lineweaver, C. H. *Science* **1999**, *284*, 1503−1507.
(25) Karplus, M.; Weaver, D. L. *Protein Sci.* **1994**, *3*, 650.
(26) (a) Wetlaufer, D. B. *Proc. Natl. Acad. Sci. U.S.A.* **1973**, *70*, 697. (b) Wetlaufer, D. B. *Trends Biochem. Sci.* **1990**, *15*, 414.
(27) Ptitsyn, O. *Nat. Struct. Biol.* **1996**, *3*, 488.

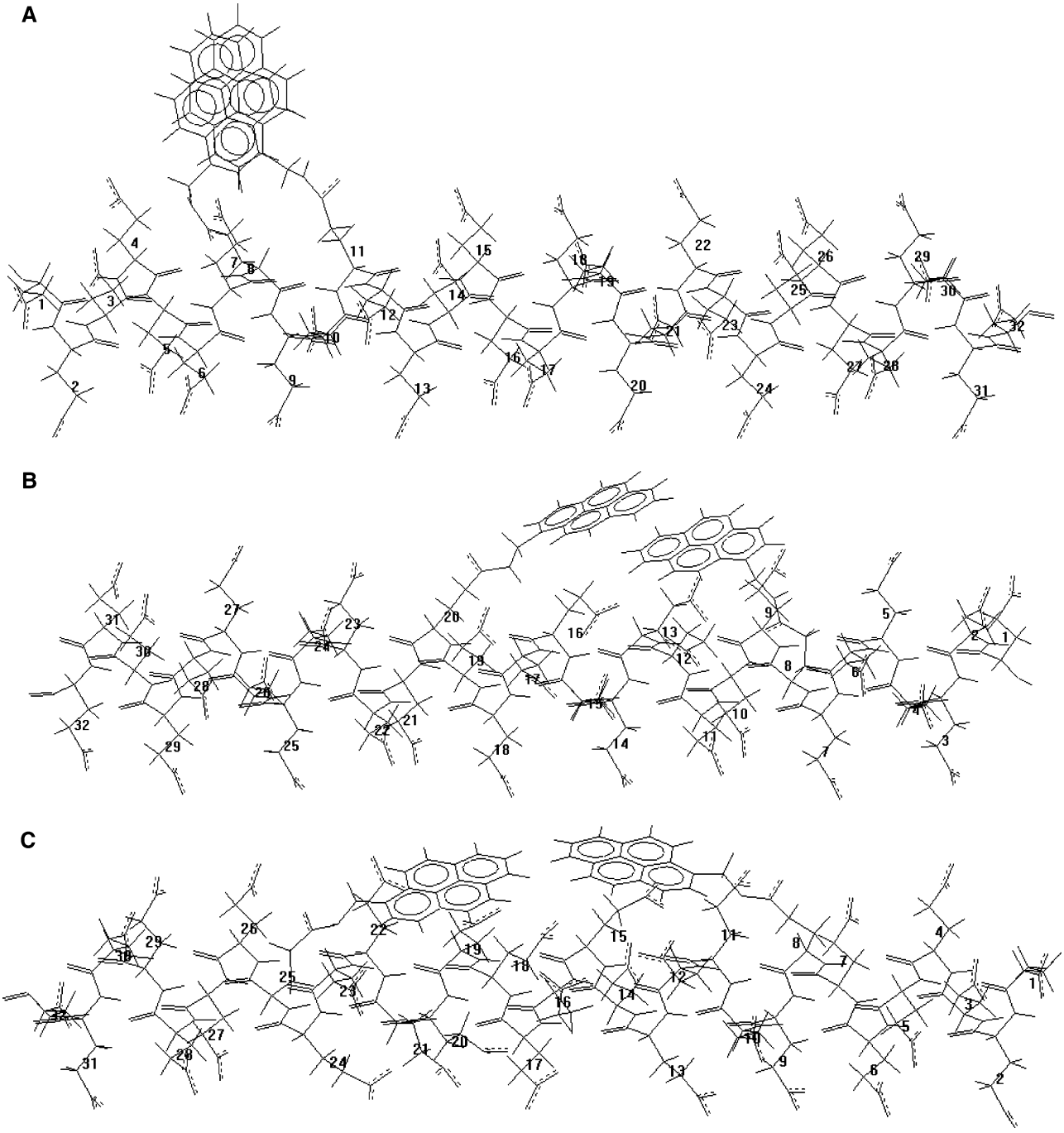

Figure 9. A: Pyrenes are located on the 8th and 11th glutamic acid residues. Nine carbon atoms of one pyrene are overlapped by the second pyrene. Good overlap. B: Pyrenes are located on the 8th and 20th glutamic acid residues. Three carbon atoms of one pyrene are overlapped by the second pyrene. Partial overlap. C: Pyrenes are located on the 8th and 25th glutamic acid residues. Between the two pyrenes, no carbons overlap.

structure was created where one 1-pyrenemethylamine pendant was attached onto the 8th glutamic acid and a second 1-pyrenemethylamine was attached on the 9th residue. A molecular mechanics optimization using the Fletcher−Reeves algorithm was performed during which the following constraints were imposed. The distances between two carbon atoms of the first pyrene molecule and the same carbon atoms of the other pyrene molecule were set to equal 3.4 Å (the typical distance between two aromatic planes such as between graphite sheets or DNA base pairs) by the end of the molecular mechanics optimization. None of the backbone atoms of the α-helix were included in the optimization, i.e., the α-helical backbone was not altered during the optimization. The side chains of the glutamic acid residues which could affect the overlap of the two pyrene moieties were included in the optimization. At the end of the optimization, the extent of overlap between the two pyrenes was estimated by calculating the number of carbon atoms of the first pyrene molecule which were covered by the frame of the second pyrene molecule. This procedure was repeated by keeping the first pyrene moiety on the 8th residue and moving the second pyrene moiety from the 9th to the 26th residue (i.e., 18 residues away from the 8th residue). The extent of overlap was qualified as good, partial, or nonexistent if the number of overlapping carbons was in the 6−9 range (cf. Figure 9A), in the 2−5 range (cf. Figure 9B), or equal to 0 (cf. Figure 9C), respectively. The extent of overlap between the two pyrenes is

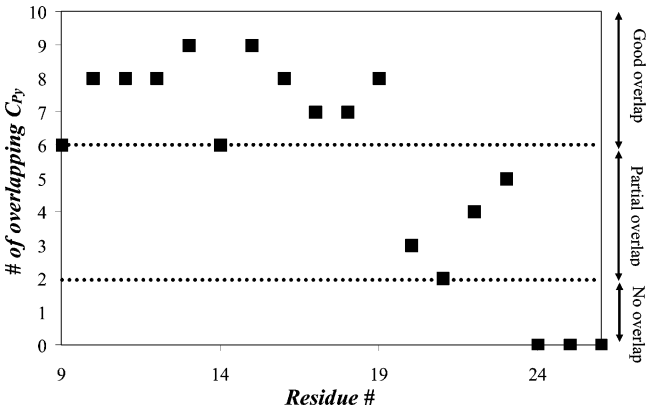

Figure 10. Number of carbon atoms C_{Py} of the two overlapping pyrene surfaces as a function of the number of amino acids separating the first pyrene located on the 8th glutamic acid and the second pyrene located on a glutamic acid located at positions 9 to 26 along the α-helical PGA.

represented as a function of the number of residues spanning the two pyrenes in Figure 10.

The results obtained from the molecular mechanics optimizations indicate that the overlap is good if the two pyrene moieties are separated by less than 11 residues, partial when the number of residues separating the two pyrenes is between 12 and 15, and nonexistent when 16 residues and more are between the two pyrenes. Figure 10 demonstrates that two pyrenes can exhibit some overlap if the glutamic acid, onto which one pyrene is attached, is flanked on both sides by a stretch of 15 glutamic acids onto any of which the second pyrene can be attached. The results from the molecular mechanics optimizations point to a blob made of $2 \times 15 + 1 = 31$ glutamic acids, in very good agreement with the N_{blob} value of 32 ± 1 obtained by fluorescence. The agreement observed between the N_{blob} value obtained experimentally and theoretically is a good indication that the blob model can be also applied to polymeric systems exhibiting some secondary structure, although it was initially derived to follow the kinetics of encounters between pyrenes randomly attached onto a random polymer coil.[3−7]

It is worth pointing out that these optimizations were performed to verify whether the geometry of the system would allow two pyrene moieties attached onto the α-helical PGA backbone to overlap. No energy considerations were taken into account since it is difficult to estimate the gain in energy provided by the formation of an excimer. An excimer is stable only while it remains exited. Furthermore, the stability of the excimer is bound to depend on the level of overlap between the two pyrenes. These details are beyond the scope of this study, which only deals with the geometry of the PyPGA system.

Conclusions

The motion of the side chain of the α-helical PGA was characterized in DMF by monitoring the fluorescence of the dye pyrene randomly attached onto the polypeptide. Excimer formation between pyrenes was possible only via the dynamic motion of the PGA side chains which probed the space surrounding them. A series of pyrene-labeled PGAs was prepared with increasing pyrene contents. As the pyrene content increased, more pyrenes attached themselves onto the polypeptide in a clustered manner. The clustering was determined from the analysis of the fluorescence decays of the pyrene monomer and excimer and confirmed by CD experiments. Simulations established that the observed pyrene clustering is due to the geometry of the α-helix. At low pyrene contents, the pyrenes are more evenly distributed along the backbone. Consequently, all trends determined as a function of pyrene content in DMF were extrapolated to a pyrene content of 0 μmol·g^{-1}, to obtain parameters which reflect the behavior of the naked polymer. In pH 9 aqueous buffer, the excimer was formed overwhelmingly by direct excitation of ground-state pyrene aggregates for all PyPGNa samples. Consequently, little information about the diffusion-controlled encounters between pyrenes could be retrieved from the fluorescence data obtained in aqueous solutions.

The number of glutamic acid units inside an α-helical PGA blob was estimated to equal 32 ± 1 in DMF. This value was found to be compatible with the geometry of the polymeric system. Molecular mechanics optimizations using the Fletcher−Reeves algorithm with Hyperchem software indicated that two pyrene moieties can exhibit some overlap as long as they are separated by less than 16 residues. Due to the symmetry exhibited by an α-helical PGA blob, a theoretical blob was estimated to equal 31 residues, in very good agreement with the N_{blob} value obtained by fluorescence. Two pyrenes attached at the tips of the PGA side chains were found to encounter with a rate constant of $0.8(\pm 0.2) \times 10^7$ s^{-1} when they are located inside the same blob.

The ability of the blob model to monitor the motion of side chains of a polymer having either a random coil or α-helical conformation is a good indication of its potential to study protein folding. The validity of the blob model, demonstrated in this and other[3−7] reports, leads to the conclusion that a residue located inside the polymer coil probes only a finite volume during the finite time the polypeptide folds into its native conformation. This postulate, whose validity has been demonstrated in organic solvents so far, could have implications on the time required for a protein to fold in aqueous solutions.

Acknowledgment. The authors thank NSERC for generous funding. J.D. is especially thankful for the financial help provided the award of a Tier-2 Canada Research Chair. J.D. is very much indebted to Professor John Honek who taught him how to use the program Hyperchem.

JA035947Q